Genome-wide single-nucleotide resolution of oxaliplatin–DNA adduct repair in drug-sensitive and -resistant colorectal cancer cell lines

Received for publication, March 5, 2020, and in revised form, April 14, 2020 Published, Papers in Press, April 16, 2020, DOI 10.1074/jbc.RA120.013347

Courtney M. Vaughn[‡], Christopher P. Selby[‡], Yanyan Yang[‡], David S. Hsu[§], and Aziz Sancar[‡1]

From the [‡]Department of Biochemistry and Biophysics, University of North Carolina School of Medicine, Chapel Hill, North Carolina 27599-7260 and the [§]Duke University Medical Center, Durham, North Carolina 27710

Edited by Patrick Sung

Platinum-based chemotherapies, including oxaliplatin, are a mainstay in the management of solid tumors and induce cell death by forming intrastrand dinucleotide DNA adducts. Despite their common use, they are highly toxic, and approximately half of cancer patients have tumors that are either intrinsically resistant or develop resistance. Previous studies suggest that this resistance is mediated by variations in DNA repair levels or net drug influx. Here, we aimed to better define the roles of nucleotide excision repair and DNA damage in platinum chemotherapy resistance by profiling DNA damage and repair efficiency in seven oxaliplatin-sensitive and three oxaliplatin-resistant colorectal cancer cell lines. We assayed DNA repair indirectly as toxicity and directly measured bulky adduct formation and removal from the genome by slot blot and repair capacity in an excision assay, and used excision repair sequencing (XR-seq) to map repair events genome-wide at single-nucleotide resolution. Using this combinatorial approach and proxies for oxaliplatin–DNA damage, we observed no significant differences in repair efficiency that could explain the relative sensitivities and chemotherapy resistances of these cell lines. In contrast, the levels of oxaliplatin-induced DNA damage were significantly lower in the resistant cells, indicating that decreased damage formation, rather than increased damage repair, is a major determinant of oxaliplatin resistance in these cell lines. XR-seq–based analysis of gene expression revealed up-regulation of membrane transport pathways in the resistant cells, and these pathways may contribute to resistance. In conclusion, additional research is needed to characterize the factors mitigating cellular DNA damage formation by platinum compounds.

Platinum-based chemotherapies are a mainstay of solid tumor treatment and are used to treat a wide array of tumors. Unfortunately, platinum therapy is very toxic and patients can experience numerous detrimental side effects including severe emesis, nephrotoxicity, ototoxicity, and neurotoxicity (1). Oxaliplatin is a first-line treatment for colorectal cancer, one of the most common forms of cancer and one of the most common causes of cancer-related deaths worldwide (2). Despite its common use, approximately half of patients have tumors are intrinsically resistant to oxaliplatin, and many initially sensitive cancers develop resistance. Patients with resistant tumors of either form endure this toxic treatment with limited or no clinical benefit (3). Thus defining mechanisms that lead to drug resistance is important for providing patients with more effective treatment options.

Platinum-based chemotherapies work by creating intrastrand dinucleotide adducts in DNA with the platinum atom covalently bound to the N7 nitrogen in adjacent guanines (4, 5). This damage is solely repaired by nucleotide excision repair (6–8). Mammalian nucleotide excision repair initiates when the XPC, RPA, and XPA factors recognize the damage and recruit the TFIIH[2] complex. Next, XPC dissociates, XPF and XPG bind to the pre-incision complex, and then the damaged strand is cleaved on the 3′ and 5′ side of the damage. The excised damage-containing DNA is then released as a single-stranded oligomer, ~24–30 nucleotides long complexed with TFIIH and XPG. DNA polymerase fills in the resulting single-stranded gap, and ligation of the nick completes repair. Excision repair of damage in the template strand of genes can also be transcription-coupled (9). In this pathway, RNA polymerase II stalls at damage sites and recruits the transcription coupling factors, CSA and CSB, which appear to assist in recruitment of the excision repair factors. Repair then proceeds following the same mechanism as in the global repair pathway. Transcription-coupled repair ensures rapid removal of transcription-blocking damage, especially damage such as platinum adducts, which are relatively slowly repaired by global repair (10).

Given that nucleotide excision repair is the sole repair mechanism for bulky intrastrand adducts, it has been widely specu-

This work was supported by National Institutes of Health Grants GM118102 and ES027255 (to A. S.) and National Institute of General Medical Sciences award 5T32 GM007092 and National Cancer Institute fellowship F30CA225060 (to C. M. V.). The authors declare that they have no conflicts of interest with the contents of this article. The content is solely the responsibility of the authors and does not necessarily represent the official views of the National Institutes of Health.

This article contains Figs. S1–S3 and Tables S1–S5.

[1] To whom correspondence should be addressed. E-mail: aziz_sancar@med.unc.edu.

[2] The abbreviations used are: TF, transcription factor; 6-4 PP, 6-4 pyrimidine-pyrimidine photoproducts; CPD, cyclobutane pyrimidine dimer; NTS, non-transcribed strand; RPKM, reads/kilobase/million total reads; TES, transcription end site; TS, transcribed strand; TSS, transcription start site; GSEA, gene set enrichment analysis; MTT, 3-(4,5-dimethylthiazol-2-yl)-2,5-diphenyltetrazolium bromide; CCAT2, colon cancer-associated transcript 2; ssDNA, single-stranded DNA; IP, immunoprecipitation; XR-seq, excision repair sequencing.

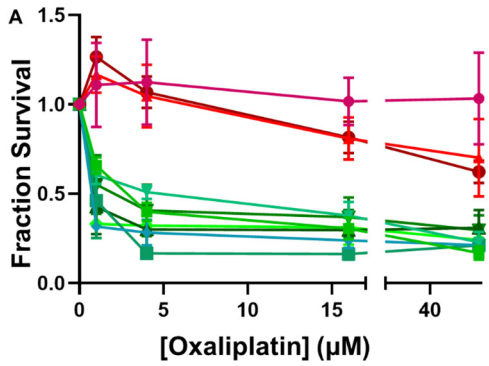

B

Cell Line	IC50 (μM)
Dld1	10.920
Sw480	7.934
Rko	7.037
Ls1034	1.592
Colo205	0.910
Hct116	0.843
Colo320hsr	0.507
Ht29	0.292
Ls174t	0.183
Ls180	0.176

Figure 1. Defining a panel of oxaliplatin-sensitive and oxaliplatin-resistant colorectal cancer cell lines. Ten colorectal cancer cell lines were tested using an MTT assay. Oxaliplatin was added to media at concentrations ranging from 0.25 to 64 μM. Four days following addition of oxaliplatin, survival was measured and normalized to an untreated control. *A,* oxaliplatin dose-response curves identified seven oxaliplatin-sensitive cell lines (*green*) and three oxaliplatin-resistant cell lines (*red*). *B,* the IC_{50} for each cell line was calculated using PRISM.

lated that increased repair efficiency would lead to platinum resistance. Many studies have explored how variation of repair at the sequence, expression, or functional level may correlate with response to platinum-based chemotherapies (11–18). However, many of the results are not reproducible and are often confounded by the multiple roles of individual proteins. Thus the link between alterations in nucleotide excision repair and response to platinum-based chemotherapies remains unclear (19, 20). In this study, we use novel methods to provide a comprehensive profile of repair efficiency for a panel of colorectal cancer cell lines that vary in oxaliplatin sensitivity by an order of magnitude. We find no link between sensitivity and repair, rather, resistant cells display diminished oxaliplatin–DNA adduct formation.

Results

Identification of oxaliplatin-sensitive and oxaliplatin-resistant cell lines

To study whether nucleotide excision repair efficiency is a determinant of oxaliplatin sensitivity, we used a panel of 10 colorectal cancer cell lines. We first tested their sensitivity to killing by oxaliplatin using the MTT cell viability assay. We treated each cell line with oxaliplatin concentrations varying from 0 to 64 μM and tested survival 4 days later. Dose-response curves clearly identified three resistant cell lines and seven sensitive cell lines (Fig. 1*A*). IC_{50} values for each cell line are shown in Fig. 1*B*. Cell line characteristics, including key driver mutations and source information are summarized in Table S1 (21, 22).

Similar oxaliplatin repair kinetics in oxaliplatin-sensitive and -resistant cell lines

To evaluate repair efficiency in the sensitive and resistant cell lines, we first examined rates of oxaliplatin removal from the genome using slot blot assays. Each cell line was incubated with 200 μM oxaliplatin for 2 h, an early damage formation time point, whereas still allowing for measurable damage levels (23). Then, the respective cell line medium was changed to be fresh and cells were incubated for an additional 0 to 34 h. The results in Fig. 2*A* show loss of oxaliplatin from the genome with time in a representative sensitive (Colo205) and resistant (Dld1) cell line. Damage levels were quantified by first normalizing the signal intensity of each damage band to its respective total amount of DNA (detected by SyberGold staining), and then calculating the fraction of damage remaining at each time point compared with 2 h. Average values for all sensitive and all resistant cell lines are plotted in Fig. 2*B*. The time for 50% of the peak initial damage to be repaired (Repair50) is listed for each cell line in Table S2. Sensitive and resistant lines show very similar repair rates, indicating that faster DNA damage repair is not a necessary component of oxaliplatin resistance.

Initial damage differs significantly between sensitive and resistant cell lines

Inspection of the oxaliplatin repair slot blots such as in Fig. 2*A* suggested uneven levels of initial damage among the cell lines. Oxaliplatin treatment is known to be influenced by factors such as drug influx, efflux, and neutralization (24–26). We therefore systematically compared the amount of initial damage incurred following treatment of each cell line with 200 μM oxaliplatin for 2 h. The results in Fig. 2*C* and Table S2 reveal substantial variations in initial damage levels. The average initial damage level was lower in resistant cells, as shown in Fig. 2*D*, furthermore, a significant, inverse correlation was found between oxaliplatin IC_{50} and initial damage level using a Pearson's correlation test (Fig. 2*E*). This association, whereas not perfect, indicates that initial damage levels contribute to cellular sensitivity. Damage levels were consistently low in the resistant lines. However, variability was seen among the sensitive lines. Several possible scenarios could explain the sensitive lines with relatively low initial damage, notably, it is possible that these two lines (Colo320hsr and Ls1034) have repair deficiencies not detected by the slot blot assay or other alterations in DNA metabolism.

Oxaliplatin-sensitive and -resistant cell lines have similar repair responses to UV irradiation

We next evaluated the role of repair on oxaliplatin sensitivity employing means to avoid the confounding factors of drug treatment mentioned above. Unlike platinums, UV irradiation rapidly and uniformly induces the intrastrand DNA diadducts cyclobutane pyrimidine dimers (CPDs) and 6-4 pyrimidine-pyrimidine photoproducts (6-4 PPs) that, like platinum-induced bulky adducts, are solely repaired by nucleotide excision repair.

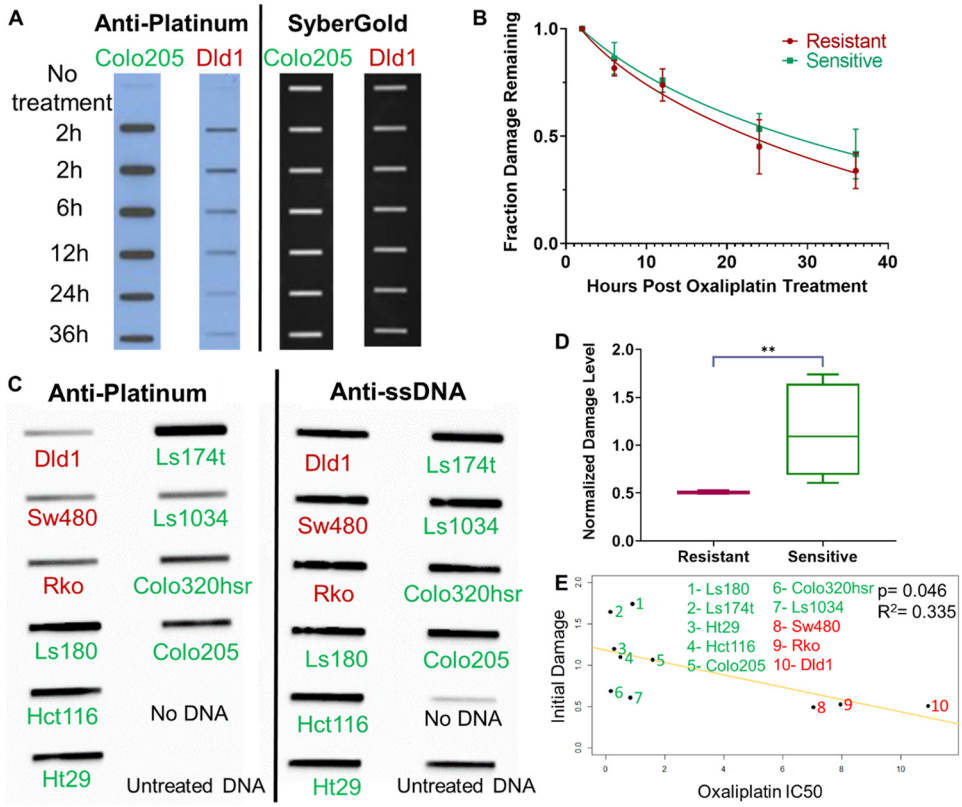

Figure 2. Oxaliplatin repair and damage formation. *A,* repair kinetics in oxaliplatin-sensitive and -resistant cell lines. Representative slot blot shows loss of damage from the genome with time following 2 h of treatment of a sensitive cell line (Colo205) and a resistant cell line (Dld1) with 200 μM oxaliplatin. Probing with anti-platinum–DNA adduct antibody (*left*) reveals the genomic DNA damage levels, and subsequent SyberGold staining of the same blot (*right*) shows the total amount of DNA blotted onto the membrane through each slot. *B,* average values for repair in the three sensitive and two resistant cell lines assayed are plotted and show no significant difference in repair rate. Two technical replicates of two biological replicates were done for each cell line. *C,* representative slot blot showing damage level following 2 h exposure of the oxaliplatin-resistant (*red*) and -sensitive (*green*) cell lines to oxaliplatin. Probing with anti-ssDNA reveals the total amount of DNA on the membrane. *D,* a plot of average initial damage levels for three resistant cell lines (*red*) and seven sensitive cell lines (*green*) shows a significant difference ($p = 0.008$, Welch's *t* test) between the two groups, indicating that a lower initial damage level correlates with resistance. *E,* a trend line fitting the IC_{50} values (*x* axis) and normalized initial damage levels (*y* axis) is plotted. A significant (Pearson's correlation, $p = 0.046$), inverse correlation again indicates that lower initial damage levels correlate with resistance.

CPDs, the predominant photoproduct, are similar to platinum adducts in that they are relatively poorly recognized and slowly repaired by the global excision repair pathway, whereas 6-4 PPs are more rapidly repaired (6). We measured the repair of UV photoproducts in our cell lines to provide a more well-controlled assessment of repair efficiency.

We first measured survival in response to UV treatment. The results in Fig. 3*A* and UV IC_{50} values in Table S2 show that whereas there is some variation in UV survival among cell lines, overall UV sensitivity is similar among cell lines, in contrast to the order of magnitude differences in sensitivity to oxaliplatin (Fig. 1*A*). Thus oxaliplatin resistance is not associated with a more resilient response to intrastrand adducts either by increased repair or decreased apoptotic signaling in response to similar initial damage levels.

We then characterized UV repair using slot blot assays to measure removal of CPD adducts from the genome. Results obtained with representative oxaliplatin-sensitive (Ls1034) and -resistant (Rko) cell lines are shown in Fig. 3*B*, and average values for the three sensitive and two resistant lines tested are shown in Fig. 3*C* (individual cell line UV Repair50 values are listed in Table S2). CPDs were removed from the genome at the same rate in sensitive and resistant cell lines.

We next used excision assays to measure the amount of excised oligomer present in cells 3 h following varying doses of UV irradiation. The excision assay uses an XPG immunoprecipitation to capture the excised, damage-containing oligomers. The oligomers are isolated, purified, labeled, and resolved on a gel. The intensity of the oligomer bands can be quantified by normalizing to a known concentration of spiked in control DNA (50-mer, Fig. 3*D*). The amount of excision product present at any given time reflects both the rate of oligomer release and concurrent degradation. Excision in representative sensitive (Hct116) and resistant (Sw480) cell lines are shown in Fig. 3*D*, and the UV dose required to obtain 50% maximum repair for each cell line is listed in Table S2. Average values for the three oxaliplatin-resistant cell lines and four sensitive cell lines tested show no difference in UV photoproduct excision as a function of dose (Fig. 3*E*). These experiments further support the finding that improved nucleotide excision repair is not a necessary component of oxaliplatin resistance.

Oxaliplatin-sensitive and oxaliplatin-resistant cell lines have similar genome-wide repair patterns

Although overall repair rates, measured by slot blot and excision assays, do not differ between oxaliplatin-sensitive and

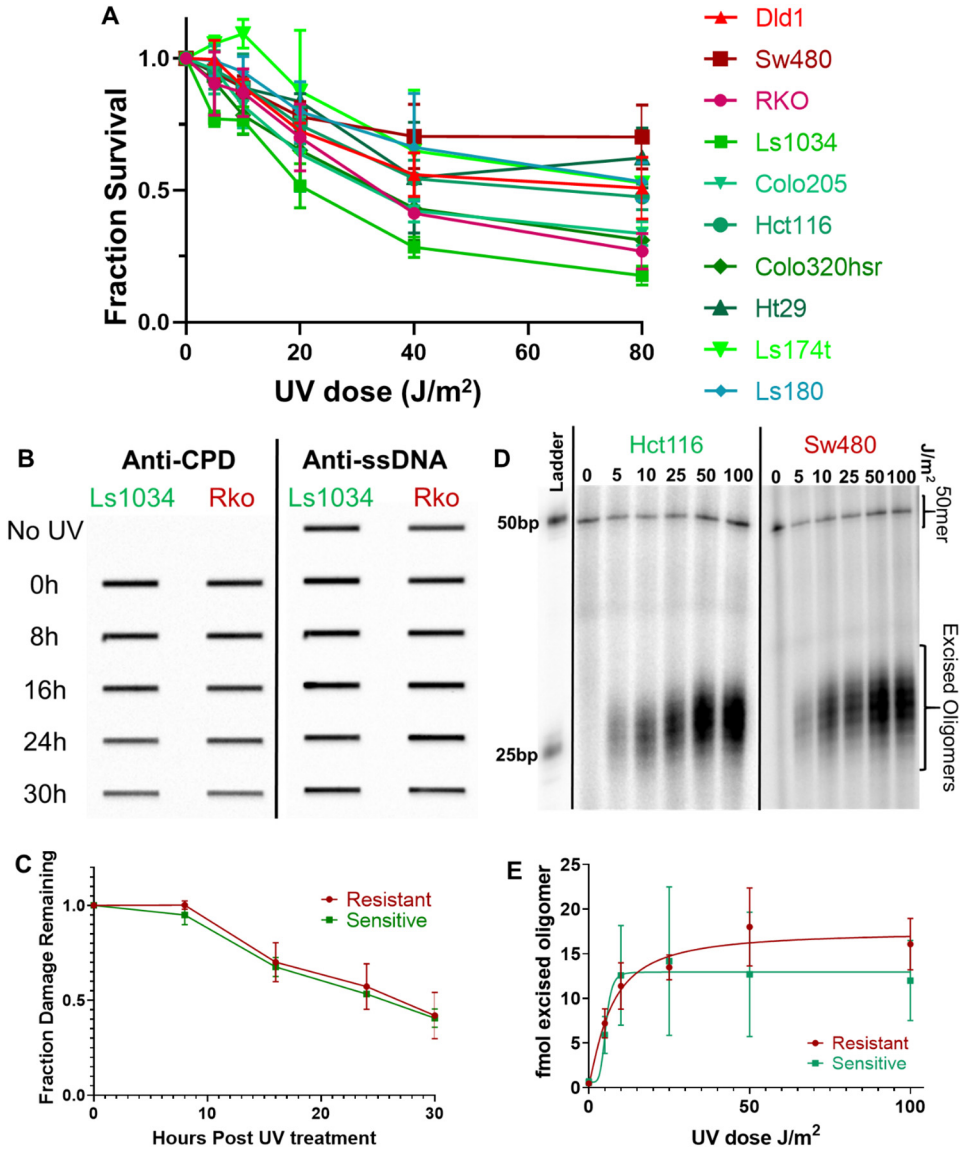

Figure 3. Repair of UV damage in oxaliplatin-sensitive and -resistant cell lines. UV creates intrastrand adducts that, like platinum intrastrand adducts, are solely removed by nucleotide excision repair. UV damage, however, is not influenced by drug influx, efflux, or neutralizing mechanisms that influence response to platinum drugs. *A,* UV survival dose-response curves for all cell lines fail to recapitulate the sensitive and resistant grouping seen with oxaliplatin survival curves. This indicates that the sensitive/resistant status of each cell line is not based on repair of intrastrand diadducts. *B,* representative slot blots ($n = 3$ blots per cell line) measuring UV-induced CPD damage levels over time are shown for a representative oxaliplatin-sensitive cell line (*Ls1034*) and a representative oxaliplatin-resistant cell line (*RKO*). Blots were probed first with anti-CPD antibody to measure damage (*left*), stripped, then probed with anti-ssDNA antibody (*right*) to measure the amount of DNA on the membrane. *C,* average damage levels, normalized to initial damage, of two oxaliplatin-resistant cell lines (*red*) and three oxaliplatin-sensitive cell lines (*green*) are plotted as a function of repair time. No difference in UV repair rate is seen between the oxaliplatin-sensitive and oxaliplatin-resistant cell lines. *D,* a representative excision assay shows similar amounts of excision product following varying doses of UV in both a representative oxaliplatin-sensitive cell line (*Hct116*) and a representative resistant cell line (*Sw480*). *E,* the average amount of excision product, measured as femtomole of excised oligo, in oxaliplatin-sensitive cell lines (*green*, $n = 4$ repeats) and oxaliplatin-resistant cell lines (*red*, $n = 3$ repeats) are plotted as a function of UV dose. No significant difference in amount of repair is seen between sensitive and resistant cell lines.

oxaliplatin-resistant cell lines, we hypothesized that resistant cell lines may, to their benefit, prioritize repair of certain genomic regions differently from sensitive cell lines. To test this hypothesis we used XR-seq after treating the cells with 200 μM oxaliplatin for 2 h (27, 28). In XR-seq, the damage-containing oligomers excised during repair are isolated and purified by sequential immunoprecipitations, first using repair protein antibodies, and then using platinum damage antibodies. The damage is then reversed and the oligomers are amplified by PCR, and sequenced. The oligomer sequences are then aligned to the genome. The result is a nucleotide level map of repair throughout the genome. The screenshot in Fig. 4*A* shows XR-seq results for a representative 250,000-kbp section of the genome. This section contains the *Dhfr* and *Msh3* genes, which are transcribed in opposite directions. Repair in each strand (plus and minus) of a representative resistant (Dld1, *red*) and sensitive (Ls180, *green*) cell line is shown. Excised oligo reads per kilobase per million total reads (RPKM, *y* axis) are represented as peaks across the gene and indicate the number of excision products found at a given location. Clearly evident in the screenshot is preferential, transcription-coupled repair of the transcribed strand (TS) of the *Dhfr* and *Msh3* genes in both

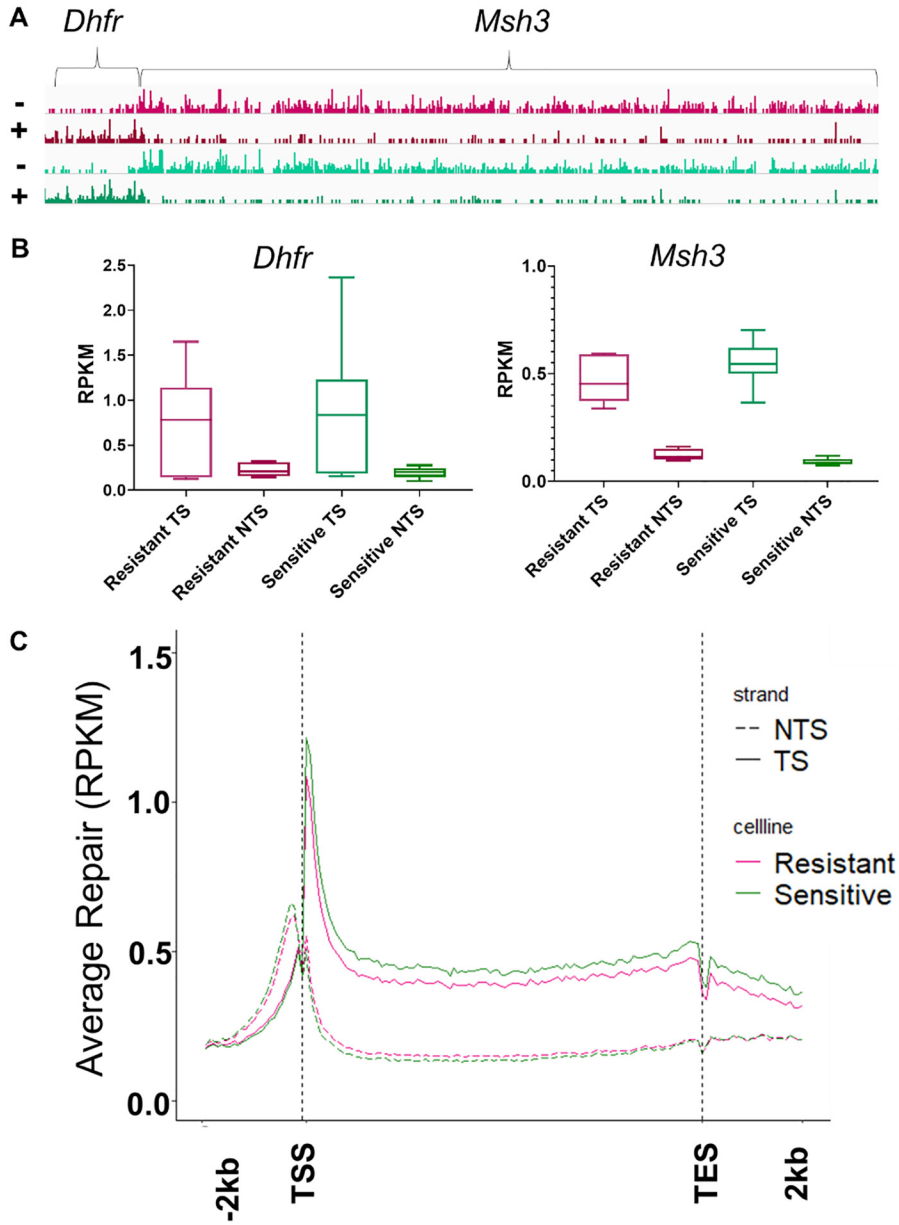

Figure 4. Oxaliplatin-sensitive and -resistant cell lines show similar genome wide repair patterns. Repair maps were created for all cell lines using XR-seq after 2 h of treatment with 200 μM oxaliplatin (2 biological replicates for all cell lines except Ls174t and Colo320hsr). *A,* representative genes, *DHFR* and *MSH3*, show similar repair levels and patterns in sensitive (*green*, Ls180) and resistant (*red*, DLD1) cell lines. Both genes have strong transcription-coupled repair as indicated by the stronger repair signal seen in the TS compared with the NTS. The minus strand is the TS in *Msh3* and the plus strand is the TS in *Dhfr*. *B,* average RPKM for the TS and NTS of DHFR and MSH3 from all XR-seq experiments show similar repair levels between all sensitive (*green*) and all resistant (*red*) cell lines. *C,* average RPKM of all resistant cell lines (*red*) and all sensitive cell lines (*green*) for all genes over 1 kbp with ≥5 kbp between genes are plotted for the TS and NTS, scaled to a unit gene. Each gene is split into 100 bins to create the *x* axis, and the average bin values for all genes are plotted as RPKM. No significant difference is seen in repair pattern or level of transcription-coupled repair.

cell lines. We quantified the RPKM for both strands of each gene, then averaged the repair values for all sensitive and resistant cell lines, and found no difference in strand-specific repair levels at any significance threshold (Fig. 4*B*).

To compare transcription-coupled repair in all genes and cell lines, we first constructed a "unit gene" for all 10 cell lines (n = 2 for all cell lines except n = 1 for Ls174t and Colo320hsr). The unit gene illustrates the average repair of each gene in a cell line. To do this, for each cell line, results for all nonoverlapping genes over 1 kbp were divided into 100 bins, and the repair level for each bin was averaged from the first bin at the transcription start site (TSS) to the last bin at the transcription end site (TES). Average repair 2 kbp upstream and downstream was also determined for each unit gene. Next, repair across the sensitive and resistant cell lines were averaged. The average unit gene repair profiles in Fig. 4*C* are similar to profiles seen in other human cell types, and in cells of other species, which show elevated TS repair, which peaks near the TSS, and largely depressed non-transcribed strand (NTS) repair, which peaks immediately upstream of the TSS and results from antisense transcription at the promoter (28–32). Fig. 4*C* shows that overall, there is no difference in amount or pattern of gene-specific repair between oxaliplatin-sensitive and oxaliplatin-resistant cell lines. This indicates that the levels of transcription-coupled repair are sim-

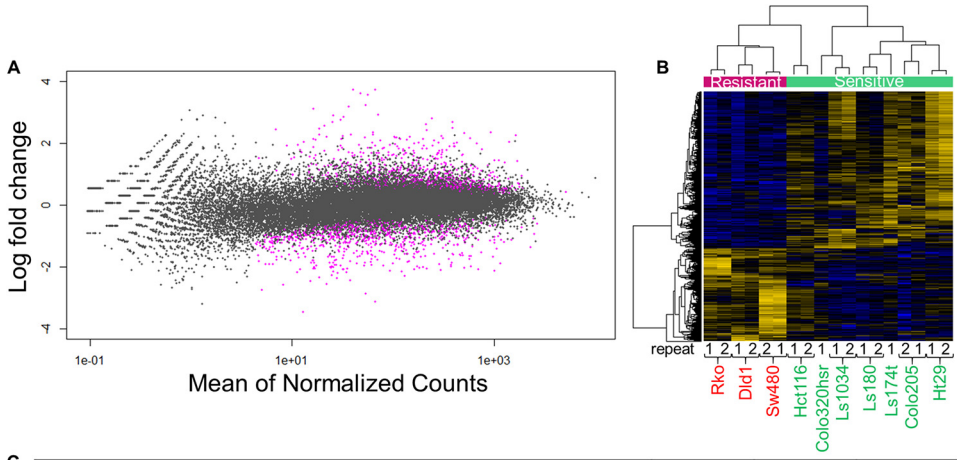

C

Top 10 Pathways Enriched in Resistant Cell Lines	SIZE	NES	FDR q-val
GO_REGULATION_OF_POTASSIUM_ION_TRANSPORT	40	2.201	0.011
GO_POSITIVE_REGULATION_OF_POTASSIUM_ION_TRANSPORT	17	2.071	0.055
GO_NEGATIVE_REGULATION_OF_ION_TRANSPORT	66	1.977	0.056
GO_ION_CHANNEL_REGULATOR_ACTIVITY	61	1.981	0.063
GO_ENDOCRINE_HORMONE_SECRETION	24	1.953	0.069
GO_REGULATION_OF_METAL_ION_TRANSPORT	172	1.935	0.069
GO_NEGATIVE_REGULATION_OF_SYNAPTIC_TRANSMISSION	29	1.987	0.069
GO_SARCOPLASMIC_RETICULUM_MEMBRANE	15	1.941	0.071
GO_CALCIUM_ION_IMPORT	35	1.913	0.071
GO_POSITIVE_REGULATION_OF_ERBB_SIGNALING_PATHWAY	18	1.920	0.071

Figure 5. Genes differentially expressed in sensitive *versus* resistant cells. Oxaliplatin-resistant cells show enrichment for membrane components and transport in resistant cells, and sensitive cells exhibit enrichment for metabolic processes. *A,* MAplot of genes shows that a small fraction of genes are significantly differentially repaired (expressed) between sensitive and resistant cell lines. For each gene (plotted as a *dot*), the difference between sensitive and resistant cell lines (log fold-change) is plotted over the average counts across all samples (mean of normalized counts). Genes exhibiting significantly different repair (expression) are plotted in *purple* (adjusted *p* values <0.05). *B,* heat map of the genes repaired differentially in sensitive (*green band*) *versus* resistant (*red band*) cell lines. *Yellow lines* indicate higher expression, whereas *blue lines* indicate lower expression. 417 genes were found to have significantly higher repair in resistant cell lines, whereas 705 genes were found to have significantly higher repair in sensitive cell lines. *R1* and *R2* denote repeats for each cell line. *C,* gene set enrichment analysis of the differentially repaired genes showed enrichment of membrane transport pathways in resistant cell lines (FDR *q*-value <25%). The top 10 most significantly enriched pathways are shown, additional pathways are in Table S1. No significantly enriched pathways (FDR *q*-value <25%) were identified from the genes up-regulated in sensitive cell lines (Table S2). *Size,* number of genes from our input in the pathway; *NES*, normalized enrichment score, the quantification of the overrepresentation of a gene set in the top or bottom of a ranked list of genes normalized for all dataset permutations; *FDR*, false discovery rate, the probability a NES score is a false-positive finding (39).

ilar in both groups. These analyses extend our observation that repair efficiency is not an essential component of oxaliplatin resistance.

Differences in gene expression in oxaliplatin-sensitive and oxaliplatin-resistant cell lines indicate a role for membrane transport in oxaliplatin resistance

Although overall, average transcription-coupled repair of all genes showed no difference in sensitive *versus* resistant cell lines (Fig. 4), we extended our analysis to detect possible differences in transcription-coupled repair within individual genes. To do this, we used the RPKM values for the TS of each gene, which reflects each gene's transcription-coupled repair level and thus gene expression level. Focusing first on individual repair genes, as shown in Fig. S1*A*, we found comparable levels of expression in sensitive and resistant cell lines, with the exception of *XPF* which, despite claims that *XPF* up-regulation correlates with platinum resistance (33), displayed higher expression in sensitive cell lines than in resistant lines. We next tested the copper efflux (*ATP7A*, *ATP7B*) and influx channels (*SLC31A1*, *SLC31A2*) that have been strongly implicated in platinum resistance (34–36). No difference in expression of these transporter genes was detected with the possible exception of *SLC31A1*. Repair of the TS of *SLC31A1* was lower in resistant lines at a *p* value of 0.015 (Welch's *t* test, Fig. S1*B*), although the association between *SLC31A1* and DNA damage in the 10 cell lines was not significant (Pearson's correlation test, Fig. S1*C*).

The above comparisons of TS repair, done on a gene-by-gene basis, were extended to compare expression of all genes in sensitive *versus* resistant cell lines using the DESeq2 analysis package (37). Among the ~30,000 genes analyzed, we identified 1122 differentially repaired genes with an adjusted *p* value less than 0.05 (Fig. 5*A*). 417 of these genes had higher repair levels in resistant cell lines compared with sensitive cell lines and 705 of the genes had higher repair levels in sensitive cell lines compared with resistant cell lines (Fig. 5*B*). One or more of these genes, listed in Table S3, could be involved in processes such as oxaliplatin transport, stability, or processing.

It is possible that resistance is determined by the outcome of several of the 1122 differentially expressed genes acting in a related manner, for example, having related functions, cellular locations, or regulation. We tested this supposition by applying gene set enrichment analysis (GSEA) of the 1122 genes. In

agreement with other studies (24, 38), our analysis found that oxaliplatin-resistant cells were enriched in gene sets including membrane transporters and channels, and their regulators, at a false discovery rate *q*-value of under 25% indicative of a low chance that these findings are false positives (Table S4) (39). Transport processes and plasma membrane components were also identified as significantly up-regulated in resistant cells using the publically available STRING database pathway analysis software (40). Among oxaliplatin-sensitive cell lines, enrichment of the cell cycle and metabolism gene sets was the strongest; however, none of these were below a 25% false discovery rate (Table S5).

We were particularly interested in understanding why the Ls1034 and Colo320hsr cell lines were sensitive even though they displayed relatively low initial damage. To this end, we first compared gene expression (as transcribed strand repair level) in these two lines with expression in the other sensitive lines (that exhibited high levels of oxaliplatin damage) by analyzing with DESeq2. 4117 differentially expressed genes were identified. Comparison of gene expression in Ls1034 and Colo320hsr with the resistant cell lines revealed 3603 differentially expressed genes. It is possible that one or more genes in these two sets contribute to relatively high toxicity of low levels of oxaliplatin–DNA damage. Inspection of these two data sets, focusing on the most differentially expressed genes yielded some provocative candidates. For example, compared with resistant cell lines, low-damage sensitive lines have 5.5× higher expression of colon cancer-associated transcript 2 (CCAT2). CCAT2 is expressed at higher levels in colorectal tumor tissue compared with adjacent healthy tissue, and promotes cancer cell proliferation by down-regulating expression of the micro RNA-145 tumor suppressor. It is linked to clinical outcome (41–44), and a functional SNP in CCAT2 has been shown to correlate with improved response to oxaliplatin (45). Thus CCAT2 may be an important factor in activating cell death in response to low initial oxaliplatin damage levels. We found other cancer-associated noncoding RNAs among the top up-regulated genes in low damage-sensitive cell lines compared with resistant cell lines (CCAT2 and CASC8) and compared with high-damage sensitive lines (CASC11, CASC8, and PCAT1), supporting a possible role for regulatory RNAs in oxaliplatin response (Fig. S2) as previously described (46). GSEA and STRING analysis of the two differentially expressed gene data sets did not yield any sets of genes associated with resistance.

Oxaliplatin-sensitive and -resistant cell lines have similar responses to mitomycin C and hydrogen peroxide

In addition to forming intrastrand diadducts, platinums induce very low levels of interstrand cross-links, and it has been proposed that these cross-links contribute to sensitivity (47). To examine the sensitivity of our cell lines to this type of DNA damage, we treated them with mitomycin C, an interstrand cross-linker, and measured cell viability 4 days later (Fig. S3*A*, Table S2). No significant correlation was found between oxaliplatin IC_{50} and mitomycin C IC_{50}, suggesting that enhanced repair of interstrand cross-links is not a common pathway in oxaliplatin resistance. Results also show that the two oxaliplatin-sensitive lines (Colo320hsr and Ls1034) that exhibited relatively low levels of oxaliplatin damage are not hypersensitive to mitomycin C, therefore, their sensitivity is unlikely due to deficient cross-link repair.

Platinating drugs may also induce reactive oxygen species that damage DNA (48). To test if oxaliplatin response correlates with response to this damage type, we treated our cell lines with hydrogen peroxide and measured viability 4 days later (Fig. S3*B*, Table S2). Although two of the three oxaliplatin-resistant cell lines were more resistant to reactive oxygen damage, the third was quite sensitive and thus there was no significant correlation between oxaliplatin IC_{50} and hydrogen peroxide IC_{50}, suggesting that enhanced repair of reactive oxygen-mediated oxaliplatin damage is not a common pathway for resistance. Again, the Colo320hsr and Ls1034 lines were not hypersensitive to hydrogen peroxide and therefore their apparent high sensitivity to oxaliplatin is probably not due to inadequate repair of oxidative damage produced by oxaliplatin.

Discussion

Enhanced excision repair capacity has been proposed as a contributing factor in cellular resistance to platinating anticancer drugs; however, the current data to support this notion are inconsistent and fail to address confounding factors (11–20). To our knowledge, ours is the most comprehensive study to address this issue, compounding multiple novel methods to create the most complete characterization of nucleotide excision repair in cancer cell lines. Notably, this is the first time excision repair maps have been generated to study drug response. This is also one of the first studies to measure the repair response to UV in the context of platinum resistance allowing us to control for confounding factors such as drug transport and additional damage types. We analyzed the excision repair capacity of seven oxaliplatin-sensitive and three oxaliplatin-resistant colorectal cancer cell lines. IC_{50} values for these lines varied by an order of magnitude, yet the measures of repair that we employed revealed no consistent association between resistance and repair. Repair measurements included slot blot assays to detect removal of both oxaliplatin and UV photoproducts from the genomes of each line. UV photoproduct repair was also measured among cell lines by excision assay, which detects the relative repair rate at the time sampled, as opposed to the slot blot assay, which detects cumulative repair at each time sampled. Oxaliplatin is known to produce interstrand cross-links at a low level, and also may damage cells by producing reactive oxygen species (47, 48). We tested response to UV, the interstrand cross-linking agent mitomycin C, and hydrogen peroxide and found that oxaliplatin response does not significantly correlate with response to any individual damage type. Finally, we assayed repair by XR-seq to detect how the different cell lines prioritize repair across the genome. Overall, repair patterns were the same in all cell lines. Interestingly, transcription-coupled repair in a small set of genes varied consistently between sensitive and resistant lines. However, these differences reflect differences in transcription, not repair *per se*. Our consistent finding that repair differences cannot account for differences in oxaliplatin response in our cell lines is further

supported by our XR-seq analysis, which showed no increased expression of repair genes in resistant cell lines.

Platinating anticancer drugs kill cells by binding to DNA. In light of our results showing that differences in DNA repair do not account for the cellular resistance we observed, it makes sense that this resistance is related to lower net influx of drug, as has been found in other studies and now is strongly supported by this study (23, 49–51). Low initial platinum levels in resistant cells are thought to arise from reduced influx and/or increased efflux of drug, and several membrane proteins have been implicated in transmembrane transport of platinum drugs (34–36). Analysis of gene expression based upon our XR-seq data support a role for one of these proteins, CTR1 (encoded by *SLC31A1*), which transports copper into the cell and was down-regulated in our resistant cells. Interestingly, our data did not support a role for the other three candidate transport proteins, rather, our data identified a novel set of membrane proteins as candidates for future study. Identifying whether any of these factors contribute to oxaliplatin resistance could improve treatment options for patients. For example, co-treatment of oxaliplatin with an inhibitor to an up-regulated oxaliplatin efflux pump could in theory render resistant cells sensitive again.

Although the initial level of DNA damage is a major determinant of oxaliplatin sensitivity, however, other factors may also contribute. Notably, sensitive lines demonstrated a relatively wide range of initial damage and two of these lines demonstrated relatively low levels of initial damage. Analysis of our XR-seq data identified several factors including cancer-associated noncoding RNAs that may contribute to the high sensitivity of these two cell lines to relatively low levels of damage.

Our data showed a wide range in response of cell lines to mitomycin C and peroxide, and it is possible that enhanced repair of interstrand cross-links and oxygen-mediated damage have a modest role in resistance to oxaliplatin in some cell lines. If enhanced repair of DNA cross-links or oxygen-mediated damage by oxaliplatin were to substantially increase resistance, then we would have observed resistant cells that demonstrate high levels of oxaliplatin damage. This was not observed. None of our cell lines showed both high resistance and high damage. Conversely, the two sensitive cell lines that exhibited relatively low levels of oxaliplatin were not hypersensitive to mitomycin C or hydrogen peroxide (Table S2), suggesting no substantial role of cross-link or oxidative damage repair in the sensitivity of these cells.

Overall, we characterized a panel of colorectal cancer cell lines to provide the most holistic view of the role of nucleotide excision repair in oxaliplatin resistance possible with current methods. All of our results support the conclusion that repair is not a necessary determinant of oxaliplatin resistance. We also show that damage levels play a major role in determining oxaliplatin treatment outcome in our cell lines; however, damage levels do not completely predict sensitivity. Additional studies are needed to determine the factors that both lead to and mitigate initial damage formation and their roles in oxaliplatin response. Our repair sequencing datasets provide a starting point to identify these factors.

Experimental procedures

Cell culture

Dld1, Rko, Ls1034, Ls180, and Colo205 cell lines were purchased from American Type Culture Collection (ATCC). Sw480, Hct116, Ht29, Colo320hsr, and Ls174t cell lines were obtained from the Tissue Culture Facility at the University of North Carolina. All cell lines used are ATCC cell lines and were grown under the conditions specified on their website. Cells were split at a 1:10 ratio when they reached 80% confluence and were never split more than 30 passages. Frozen stocks for each cell line were made on the second and third passages. Cell culture and drug treatments were conducted at 37 °C in 5% CO_2.

Oxaliplatin survival

All survival studies were conducted in 96-well Corning Costar plates using the Promega MTT assay. Cells were plated at 5,000 cells/well 24 h prior to treatment with oxaliplatin. Oxaliplatin from TSZChem was first dissolved as a 6.4 M stock in DMSO (made fresh before each biological replicate), and then diluted to a 640 μM solution using the culture media appropriate for each cell line. Serial dilutions in the respective culture media were performed to obtain solutions with 160, 40, 10, and 2.5 μM oxaliplatin. Solutions were then added to the wells at a 1:10 ratio such that cells were ultimately treated with 64, 16, 4, 1, 0.25, or 0 μM. For every cell line, three technical repeats of each dose were conducted for each of the three biological replicates. Four days after the addition of oxaliplatin to the media, MTT dye was added to the media. Three hours after the addition of dye, the media was replaced with solubilizer solution. Dye intensity was read using a Spectra Max M3 plate reader and SoftMax® Pro 6 microplate reader control and data analysis software. The three technical repeats for each dose were averaged and normalized to the signal from the untreated control. Graph Pad Prism 8 software was used to plot dose-response and determine IC_{50}.

UV survival

Survival following irradiation with principally 254-nm UV light was conducted following the same protocol as oxaliplatin survival with the following exceptions. Cells were plated at 50,000 cells/well 24 h prior to treatment. Immediately before UV irradiation, media was removed and wells were washed with PBS to eliminate any effect of culture media on UV treatment. Fresh media was added to each well following treatment. One 96-well–plate was used for each UV dose (0, 5, 10, 20, 40, and 80 J/m^2). Irradiations took 80 s or less at the dose rate used. Survival was measured 1 day after UV treatment rather than 4 days.

Mitomycin C and hydrogen peroxide survival

These survival assays were conducted following the same protocol as the oxaliplatin survival studies with the following exceptions: mitomycin C was first diluted to a 5 M stock in DMSO. This 5 M stock was then diluted for each biological replicate using the appropriate culture media to make 40 μM solution and was then serially diluted to make solutions with 20, 10, 5, and 2.5 μM concentrations. Hydrogen peroxide came as a 30% solution and was diluted to 640 μM concentration in the

appropriate culture media. Serial dilutions in media were then made to create solutions with 160, 40, 10, and 2.5 μM. Both mitomycin C and hydrogen peroxide solutions were added to wells at a 1:10 ratio.

Oxaliplatin slot blot (31, 52)

Cells were plated in 100-mm round dishes. Cells were treated with 200 μM oxaliplatin for 2 h once they reached ~100% confluence to eliminate damage level reduction due to cell divisions. After a 2-h treatment period, culture media was changed and cells were then either washed with ice-cold PBS and collected, or incubated for an additional 4, 10, 22, or 34 h to allow for repair before collection. DNA was extracted using the QIAamp DNA mini kit. DNA was then treated with RNase A for 1 h and purified using a Qiagen PCR purification kit. DNA was quantified and diluted such that 150 ng of each DNA sample was loaded into each well of a slot blot apparatus for repair kinetics experiments, and 250 ng of DNA was loaded into each well for initial damage experiments. DNA was then transferred to a membrane, and blots were blocked in PBS with 0.1% Tween (PBS-T) and 5% milk at 4 °C overnight. The next day the blots were washed in PBS-T three times, and incubated in Abcam anti-platinum damage primary antibody (AbCam, 1:10,000 in PBS-T) at 4 °C overnight. Blots were washed and incubated in GE Healthcare anti-rat IgG conjugated to horseradish peroxidase for 2 h. Bio-Rad Clarity™ Western ECL Substrates were used to detect signal, and the signal was quantified using ImageQuant. DNA loading was detected with either an antibody against ssDNA or with SyberGold. For the repair kinetic study, two technical replicates were done for each of two biological replicates for each cell line. For the initial damage experiments, two technical replicates of three biological repeats were conducted for each cell line. GraphPad Prism 8 software was used to plot damage amount and to calculate repair values.

UV slot blot

UV slot blot was conducted following the same protocol as oxaliplatin slot blot with the following exceptions. Immediately before UV irradiation, media was removed and cells were washed with PBS. Cells were treated with 25 J/m^2 and fresh media was added following treatment. Three biological replicates were conducted for each cell line tested.

Excision assay (8, 53)

Cells were plated in one 150-mm round dish per dose and allowed to grow to ~100% confluence. Immediately before UV irradiation, media was removed and cells were washed with PBS. Cells were then irradiated with 0, 5, 10, 25, 50, or 100 J/m^2. Fresh media was added following irradiation, and plates were returned to the incubator for a 3-h repair incubation. Cells were harvested in cold PBS, suspended in a lysis buffer without SDS, and lysed using a homogenizer. Excised oligomers were isolated from the soluble fraction of homogenates by XPG antibody (Santa Cruz Biotechnology) immunoprecipitation. During the elution of the XPG IP, "spike" control DNA (2 fmol) was added to each sample. The control spike DNA was an undamaged 50-mer oligomer used to monitor subsequent DNA recovery and labeling efficiency. At this point samples containing control and excised DNA were extracted with phenol-chloroform, precipitated with ethanol, labeled with ^{32}P-cordecepin, and run on a sequencing gel. The gels were exposed to a phosphorimager screen and imaged with the Typhoon detection system. Signal was measured using ImageJ software. GraphPad Prism 8 software was used to plot excised oligo amount and calculate repair values. At least four biological replicates were conducted for each cell line tested.

XR-seq (27, 28)

Cells were plated in 150-mm round dishes and allowed to grow to ~100% confluence. The number of plates needed varied by cell line. They were then exposed to 200 μM oxaliplatin for 2 h and then washed with cold PBS and collected. Cells were suspended in lysis buffer without SDS and lysed using a homogenizer. Excised oligomers were isolated from the soluble fraction of homogenates by XPG antibody (Santa Cruz Biotechnology) immunoprecipitation. The oligomers were then eluted, purified, annealed, and ligated to adaptors. A second IP for platinum damage was then performed to further purify the excised oligomers. The platinum damage was then reversed with sodium cyanide. PCR amplification (15 cycles or fewer) and gel purification were then conducted and samples were sequenced using NextGen sequencing. XR-seq was conducted for two biological replicates for all cell lines, except Colo320hsr and Ls174t, for a total of 18 libraries. Sequences were aligned to the hg38_UCSC genome and read counts/gene were determined. Each sample had at least 6.8 million unique mapped reads. Repair patterns were visualized using the Integrated Genome Viewer from the Broad Institute. Average repair patterns for a unit gene was determined and plotted as described (31, 32). Repair read counts from the transcribed strands of genes were analyzed with the DESeq2 package in R to determine genes with significant differential repair. GSEA software from the Broad Institute and STRING (SIB, CPR, EMBL) were used to determine enriched processes for differentially repaired genes.

Data availability

The raw data and alignment data have been deposited in the Gene Expression Omnibus under accession number GSE146473.

Author contributions—C. M. V., C. P. S., D. S. H., and A. S. conceptualization; C. M. V. and C. P. S. data curation; C. M. V., C. P. S., Y. Y., and D. S. H. formal analysis; C. M. V. and A. S. supervision; C. M. V., C. P. S., and A. S. funding acquisition; C. M. V., C. P. S., and A. S. investigation; C. M. V. and C. P. S. visualization; C. M. V., C. P. S., Y. Y., D. S. H., and A. S. methodology; C. M. V. and C. P. S. writing-original draft; C. M. V. and A. S. project administration; C. M. V., C. P. S., Y. Y., D. S. H., and A. S. writing-review and editing; D. S. H. and A. S. resources.

References

1. Ho, G. Y., Woodward, N., and Coward, J. I. (2016) Cisplatin versus carboplatin: comparative review of therapeutic management in solid malignancies. *Crit. Rev. Oncol. Hematol.* **102,** 37–46 CrossRef Medline
2. Benson, A. B., 3rd, Venook, A. P., Cederquist, L., Chan, E., Chen, Y. J., Cooper, H. S., Deming, D., Engstrom, P. F., Enzinger, P. C., Fichera, A., Grem, J. L., Grothey, A., Hochster, H. S., Hoffe, S., Hunt, S., *et al.* (2017)

Colon cancer, version 1.2017, NCCN clinical practice guidelines in oncology. *J. Natl. Compr. Canc. Netw.* **15,** 370–398 CrossRef Medline
3. de Gramont, A., Schmoll, H. J., Cervantes, A., and Tournigand, C. (2003) The evolving role of oxaliplatin in the management of colorectal cancer. *Colorectal Dis.* **5,** 10–19 CrossRef Medline
4. Wang, D., and Lippard, S. J. (2005) Cellular processing of platinum anticancer drugs. *Nat. Rev. Drug Discov.* **4,** 307–320 CrossRef Medline
5. Hall, M. D., Okabe, M., Shen, D. W., Liang, X. J., and Gottesman, M. M. (2008) The role of cellular accumulation in determining sensitivity to platinum-based chemotherapy. *Annu. Rev. Pharmacol. Toxicol.* **48,** 495–535 CrossRef Medline
6. Sancar, A. (1996) DNA excision repair. *Annu. Rev. Biochem.* **65,** 43–81 CrossRef Medline
7. Wood, R. D. (1997) Nucleotide excision repair in mammalian cells. *J. Biol. Chem.* **272,** 23465–23468 CrossRef Medline
8. Kemp, M. G., Reardon, J. T., Lindsey-Boltz, L. A., and Sancar, A. (2012) Mechanism of release and fate of excised oligonucleotides during nucleotide excision repair. *J. Biol. Chem.* **287,** 22889–22899 CrossRef Medline
9. Hanawalt, P. C., and Spivak, G. (2008) Transcription-coupled DNA repair: two decades of progress and surprises. *Nat. Rev. Mol. Cell Biol.* **9,** 958–970 CrossRef Medline
10. Sancar, A. (2016) Mechanisms of DNA repair by photolyase and excision nuclease (Nobel Lecture). *Angew Chem. Int. Ed. Engl.* **55,** 8502–8527 CrossRef Medline
11. Masuda, H., Ozols, R. F., Lai, G. M., Fojo, A., Rothenberg, M., and Hamilton, T. C. (1988) Increased DNA repair as a mechanism of acquired resistance to cis-diamminedichloroplatinum (II) in human ovarian cancer cell lines. *Cancer Res.* **48,** 5713–5716 Medline
12. Wu, X., Fan, W., Xu, S., and Zhou, Y. (2003) Sensitization to the cytotoxicity of cisplatin by transfection with nucleotide excision repair gene xeroderma pigmentosun group A antisense RNA in human lung adenocarcinoma cells. *Clin. Cancer Res.* **9,** 5874–5879 Medline
13. Fang, C., Chen, Y. X., Wu, N. Y., Yin, J. Y., Li, X. P., Huang, H. S., Zhang, W., Zhou, H. H., and Liu, Z. Q. (2017) MiR-488 inhibits proliferation and cisplatin sensibility in non-small-cell lung cancer (NSCLC) cells by activating the eIF3a-mediated NER signaling pathway. *Sci. Rep.* **7,** 40384 CrossRef Medline
14. Yu, W. K., Wang, Z., Fong, C. C., Liu, D., Yip, T. C., Au, S. K., Zhu, G., and Yang, M. (2017) Chemoresistant lung cancer stem cells display high DNA repair capability to remove cisplatin-induced DNA damage. *Br. J. Pharmacol.* **174,** 302–313 CrossRef Medline
15. Barckhausen, C., Roos, W. P., Naumann, S. C., and Kaina, B. (2014) Malignant melanoma cells acquire resistance to DNA interstrand cross-linking chemotherapeutics by p53-triggered upregulation of DDB2/XPC-mediated DNA repair. *Oncogene* **33,** 1964–1974 CrossRef Medline
16. Huang, Y., Wang, X., Niu, X., Wang, X., Jiang, R., Xu, T., Liu, Y., Liang, L., Ou, X., Xing, X., Li, W., and Hu, C. (2017) EZH2 suppresses the nucleotide excision repair in nasopharyngeal carcinoma by silencing XPA gene. *Mol. Carcinog.* **56,** 447–463 CrossRef Medline
17. Modi, S., Kir, D., Giri, B., Majumder, K., Arora, N., Dudeja, V., Banerjee, S., and Saluja, A. K. (2016) Minnelide overcomes oxaliplatin resistance by downregulating the DNA repair pathway in pancreatic cancer. *J. Gastrointest. Surg.* **20,** 13–23; discussion 23–14 CrossRef Medline
18. Di Francia, R., De Lucia, L., Di Paolo, M., Di Martino, S., Del Pup, L., De Monaco, A., Lleshi, A., and Berretta, M. (2015) Rational selection of predictive pharmacogenomics test for the Fluoropyrimidine/Oxaliplatin based therapy. *Eur. Rev. Med. Pharmacolog. Sci.* **19,** 4443–4454 Medline
19. Saintas, E., Abrahams, L., Ahmad, G. T., Ajakaiye, A. M., AlHumaidi, A. S., Ashmore-Harris, C., Clark, I., Dura, U. K., Fixmer, C. N., Ike-Morris, C., Mato Prado, M., McCullough, D., Mishra, S., Schöler, K. M., Timur, H., *et al.* (2017) Acquired resistance to oxaliplatin is not directly associated with increased resistance to DNA damage in SK-N-ASrOXALI4000, a newly established oxaliplatin-resistant sub-line of the neuroblastoma cell line SK-N-AS. *PLoS ONE* **12,** e0172140 CrossRef Medline
20. Bowden, N. A. (2014) Nucleotide excision repair: why is it not used to predict response to platinum-based chemotherapy? *Cancer Lett.* **346,** 163–171 CrossRef Medline
21. Ahmed, D., Eide, P. W., Eilertsen, I. A., Danielsen, S. A., Eknæs, M., Hektoen, M., Lind, G. E., and Lothe, R. A. (2013) Epigenetic and genetic features of 24 colon cancer cell lines. *Oncogenesis* **2,** e71–e71 CrossRef Medline
22. Novakovic, P., Stempak, J. M., Sohn, K.-J., and Kim, Y.-I. (2006) Effects of folate deficiency on gene expression in the apoptosis and cancer pathways in colon cancer cells. *Carcinogenesis* **27,** 916–924 Medline
23. Unger, F. T., Klasen, H. A., Tchartchian, G., de Wilde, R. L., and Witte, I. (2009) DNA damage induced by cis- and carboplatin as indicator for *in vitro* sensitivity of ovarian carcinoma cells. *BMC Cancer* **9,** 359 CrossRef Medline
24. Mezencev, R., Matyunina, L. V., Wagner, G. T., and McDonald, J. F. (2016) Acquired resistance of pancreatic cancer cells to cisplatin is multifactorial with cell context-dependent involvement of resistance genes. *Cancer Gene Ther.* **23,** 446–453 CrossRef Medline
25. Massari, F., Santoni, M., Ciccarese, C., Brunelli, M., Conti, A., Santini, D., Montironi, R., Cascinu, S., and Tortora, G. (2015) Emerging concepts on drug resistance in bladder cancer: implications for future strategies. *Crit. Rev. Oncol. Hematol.* **96,** 81–90 CrossRef Medline
26. Fang, Y., Zhang, C., Wu, T., Wang, Q., Liu, J., and Dai, P. (2017) Transcriptome sequencing reveals key pathways and genes associated with cisplatin resistance in lung adenocarcinoma A549 cells. *PLoS ONE* **12,** e0170609 CrossRef Medline
27. Hu, J., Li, W., Adebali, O., Yang, Y., Oztas, O., Selby, C. P., and Sancar, A. (2019) Genome-wide mapping of nucleotide excision repair with XR-seq. *Nat. Protoc.* **14,** 248–282 CrossRef Medline
28. Hu, J., Adar, S., Selby, C. P., Lieb, J. D., and Sancar, A. (2015) Genome-wide analysis of human global and transcription-coupled excision repair of UV damage at single-nucleotide resolution. *Genes Dev.* **29,** 948–960 CrossRef Medline
29. Oztas, O., Selby, C. P., Sancar, A., and Adebali, O. (2018) Genome-wide excision repair in *Arabidopsis* is coupled to transcription and reflects circadian gene expression patterns. *Nat. Commun.* **9,** 1503 CrossRef Medline
30. Li, W., Adebali, O., Yang, Y., Selby, C. P., and Sancar, A. (2018) Single-nucleotide resolution dynamic repair maps of UV damage in *Saccharomyces cerevisiae* genome. *Proc. Natl. Acad. Sci. U.S.A.* **115,** E3408–E3415 CrossRef Medline
31. Yang, Y., Liu, Z., Selby, C. P., and Sancar, A. (2019) Long-term, genome-wide kinetic analysis of the effect of the circadian clock and transcription on the repair of cisplatin-DNA adducts in the mouse liver. *J. Biol. Chem.* **294,** 11960–11968 CrossRef Medline
32. Deger, N., Yang, Y., Lindsey-Boltz, L. A., Sancar, A., and Selby, C. P. (2019) Drosophila, which lacks canonical transcription-coupled repair proteins, performs transcription-coupled repair. *J. Biol. Chem.* **294,** 18092–18098 CrossRef Medline
33. Guffanti, F., Fratelli, M., Ganzinelli, M., Bolis, M., Ricci, F., Bizzaro, F., Chilà, R., Sina, F. P., Fruscio, R., Lupia, M., Cavallaro, U., Cappelletti, M. R., Generali, D., Giavazzi, R., and Damia, G. (2018) Platinum sensitivity and DNA repair in a recently established panel of patient-derived ovarian carcinoma xenografts. *Oncotarget* **9,** 24707–24717 Medline
34. Howell, S. B., Safaei, R., Larson, C. A., and Sailor, M. J. (2010) Copper transporters and the cellular pharmacology of the platinum-containing cancer drugs. *Mol. Pharmacol.* **77,** 887–894 CrossRef Medline
35. Katano, K., Kondo, A., Safaei, R., Holzer, A., Samimi, G., Mishima, M., Kuo, Y. M., Rochdi, M., and Howell, S. B. (2002) Acquisition of resistance to cisplatin is accompanied by changes in the cellular pharmacology of copper. *Cancer Res.* **62,** 6559–6565 Medline
36. Samimi, G., Safaei, R., Katano, K., Holzer, A. K., Rochdi, M., Tomioka, M., Goodman, M., and Howell, S. B. (2004) Increased expression of the copper efflux transporter ATP7A mediates resistance to cisplatin, carboplatin, and oxaliplatin in ovarian cancer cells. *Clin. Cancer Res.* **10,** 4661–4669 CrossRef Medline
37. Love, M. I., Huber, W., and Anders, S. (2014) Moderated estimation of fold change and dispersion for RNA-seq data with DESeq2. *Genome Biol.* **15,** 550 CrossRef Medline
38. Meynard, D., Le Morvan, V., Bonnet, J., and Robert, J. (2007) Functional analysis of the gene expression profiles of colorectal cancer cell lines in

relation to oxaliplatin and cisplatin cytotoxicity. *Oncol. Rep.* **17,** 1213–1221 Medline

39. Subramanian, A., Tamayo, P., Mootha, V. K., Mukherjee, S., Ebert, B. L., Gillette, M. A., Paulovich, A., Pomeroy, S. L., Golub, T. R., Lander, E. S., and Mesirov, J. P. (2005) Gene set enrichment analysis: a knowledge-based approach for interpreting genome-wide expression profiles. *Proc. Natl. Acad. Sci. U.S.A.* **102,** 15545–15550 CrossRef
40. Szklarczyk, D., Morris, J. H., Cook, H., Kuhn, M., Wyder, S., Simonovic, M., Santos, A., Doncheva, N. T., Roth, A., Bork, P., Jensen, L. J., and von Mering, C. (2017) The STRING database in 2017: quality-controlled protein-protein association networks, made broadly accessible. *Nucleic Acids Res.* **45,** D362–D368 CrossRef Medline
41. Zhang, J., Jiang, Y., Zhu, J., Wu, T., Ma, J., Du, C., Chen, S., Li, T., Han, J., and Wang, X. (2017) Overexpression of long non-coding RNA colon cancer-associated transcript 2 is associated with advanced tumor progression and poor prognosis in patients with colorectal cancer. *Oncol. Lett.* **14,** 6907–6914 Medline
42. Ozawa, T., Matsuyama, T., Toiyama, Y., Takahashi, N., Ishikawa, T., Uetake, H., Yamada, Y., Kusunoki, M., Calin, G., and Goel, A. (2017) CCAT1 and CCAT2 long noncoding RNAs, located within the 8q.24.21 "gene desert", serve as important prognostic biomarkers in colorectal cancer. *Ann. Oncol.* **28,** 1882–1888 CrossRef Medline
43. Chen, S., Wu, H., Lv, N., Wang, H., Wang, Y., Tang, Q., Shao, H., and Sun, C. (2016) LncRNA CCAT2 predicts poor prognosis and regulates growth and metastasis in small cell lung cancer. *Biomed. Pharmacother.* **82,** 583–588 CrossRef Medline
44. Ling, H., Spizzo, R., Atlasi, Y., Nicoloso, M., Shimizu, M., Redis, R. S., Nishida, N., Gafà, R., Song, J., Guo, Z., Ivan, C., Barbarotto, E., De Vries, I., Zhang, X., Ferracin, M., *et al*. (2013) CCAT2, a novel noncoding RNA mapping to 8q24, underlies metastatic progression and chromosomal instability in colon cancer. *Genome Res.* **23,** 1446–1461 CrossRef Medline
45. Gong, W. J., Yin, J. Y., Li, X. P., Fang, C., Xiao, D., Zhang, W., Zhou, H. H., Li, X., and Liu, Z. Q. (2016) Association of well-characterized lung cancer lncRNA polymorphisms with lung cancer susceptibility and platinum-based chemotherapy response. *Tumour. Biol.* **37,** 8349–8358 CrossRef Medline
46. Hahne, J. C., and Valeri, N. (2018) Non-coding RNAs and resistance to anticancer drugs in gastrointestinal tumors. *Front. Oncol.* **8,** 226–226 CrossRef Medline
47. Johnson, S. W., Perez, R. P., Godwin, A. K., Yeung, A. T., Handel, L. M., Ozols, R. F., and Hamilton, T. C. (1994) Role of platinum-DNA adduct formation and removal in cisplatin resistance in human ovarian cancer cell lines. *Biochem. Pharmacol.* **47,** 689–697 CrossRef Medline
48. Preston, T. J., Henderson, J. T., McCallum, G. P., and Wells, P. G. (2009) Base excision repair of reactive oxygen species-initiated 7,8-dihydro-8-oxo-2′-deoxyguanosine inhibits the cytotoxicity of platinum anticancer drugs. *Mol. Cancer Ther.* **8,** 2015–2026 CrossRef Medline
49. Kim, E. S., Lee, J. J., He, G., Chow, C. W., Fujimoto, J., Kalhor, N., Swisher, S. G., Wistuba, I. I., Stewart, D. J., and Siddik, Z. H. (2012) Tissue platinum concentration and tumor response in non-small-cell lung cancer. *J. Clin. Oncol.* **30,** 3345–3352 CrossRef Medline
50. Veal, G. J., Dias, C., Price, L., Parry, A., Errington, J., Hale, J., Pearson, A. D., Boddy, A. V., Newell, D. R., and Tilby, M. J. (2001) Influence of cellular factors and pharmacokinetics on the formation of platinum-DNA adducts in leukocytes of children receiving cisplatin therapy. *Clin. Cancer Res.* **7,** 2205–2212 Medline
51. Wang, S., Scharadin, T. M., Zimmermann, M., Malfatti, M. A., Turteltaub, K. W., de Vere White, R., Pan, C.-X., and Henderson, P. T. (2018) Correlation of platinum cytotoxicity to drug-DNA adduct levels in a breast cancer cell line panel. *Chem. Res. Toxicol.* **31,** 1293–1304 CrossRef Medline
52. Riou, L., Eveno, E., van Hoffen, A., van Zeeland, A. A., Sarasin, A., and Mullenders, L. H. (2004) Differential repair of the two major UV-induced photolesions in trichothiodystrophy fibroblasts. *Cancer Res.* **64,** 889–894 CrossRef Medline
53. Hu, J., Choi, J. H., Gaddameedhi, S., Kemp, M. G., Reardon, J. T., and Sancar, A. (2013) Nucleotide excision repair in human cells: fate of the excised oligonucleotide carrying DNA damage *in vivo*. *J. Biol. Chem.* **288,** 20918–20926 CrossRef Medline